






# A Modified Model-Based Resistance Estimation of Lithium-Ion Batteries Using Unscented Kalman Filter

Jing-Long Chen  and Ri-Xin Wang  

Deep Space Exploration Research Center, Harbin Institute of Technology,  
Harbin, China  
wangrxhit@163.com

**Abstract.** Lithium-ion batteries are critical components for satellite, and it is necessary to monitor their state of health (SOH). At present, the most common Ah-count method in satellite has errors in long-term health monitoring. Therefore, in this work, resistance is adopted to describe SOH and a resistance estimation method is developed based on unscented Kalman filtering (UKF). To reduce the impact of unstable work condition and battery aging, a simplified electrochemistry model of lithium-ion batteries is built to replace equivalent circuit model (ECM) in UKF. In consideration of battery aging, a linear lithium ions loss model is used in this model. Then, the linear relationship between resistance and capacity is analyzed to demonstrate the ability for SOH description by resistance. Experimental data suggests that this model can effectively track the resistance in discharge process and yield satisfactory results with battery aging. Besides, this method is applicable to estimating battery SOH, as suggested by the linear relationship between estimation of resistance and actual measurements of capacity.

**Keywords:** Lithium-ion battery · Resistance estimation · Unscented Kalman filter · State of health

## 1 Introduction

Satellite is critical for communication, navigation, and military in modern society. As the core of energy source and storage component in satellite, battery would determine the life span of satellite. Lithium-ion batteries are becoming the broadest choice in satellite power system due to high-energy density and long lifetime. At present, lithium-ion batteries have been applied in new satellites by United States and European Space Agency (ESA) [1, 2]. Besides, lithium-ion batteries are also selected as Chinese third-generation satellite power storage batteries to replace NiMH and NiCd batteries. Compared to NiMH battery, lithium-ion battery requires more accurate battery manager system (BMS) to ensure the normal operation of satellite system and extend the service life [3]. The core of achieving BMS function is to monitor SOH accurately. The commonly used battery health index (HI) includes capacity, resistance, and an indirect HI. Capacity reflects SOH directly, but changes with work-condition-like temperature and varying discharge rate in practical. Otherwise, discharge capacity measurement

requires battery to discharge from fully charged state to cut-off voltage. Indirect HI is estimated capacity through data future point, including constant-voltage current charging time [4], interval capacity [5], feature points of differential voltage analysis (DVA) and incremental capacity analysis (ICA) [6–8]. These indirect HI can estimate SOH accuracy, but require voltage data under time-invariant currents. Above-mentioned HI is hard to apply in satellite because their special requirements cannot be satisfied in orbital satellite generally. Resistance is inherent character of battery and can be measured directly or estimated through measured battery signals (voltage, current and temperature). It is insensitive to discharge rate and has steady relationship with capacity. The relationship between resistance and SOH has been studied extensively. Maheshwari et al. [9] study the degradation characteristic of lithium-ion battery impedance with cycle aging based on test date. Chen et al. [10] analyze the relationship between internal resistance increases and capacity decreases, and define SOH directly according to internal resistance. Resistance in these researches is measured by dedicated devices which are hard to install on satellite. Cui et al. [11] investigate the real-time relationship between impedance and battery cycle and propose a method in which rapid identification of the impedance is built on charge and discharge curves. In this method, the calculation of transfer impedance is very complex, and the calculation of internal impedance ignore the error derived from varied SOC.

Generally, current-pulse technique and electrochemical impedance (EIS) are major approaches to measure battery internal resistance. Current-pulse technique offers a current pulse ( $\Delta I$ ) for battery and measures the voltage drop ( $\Delta V$ ). Then the resistance, also known as direct current resistance (DCR) in this case, can be calculated by  $R = \Delta V / \Delta I$ . This technique is superior for simple online implementation, yet is hard to apply in satellite directly for requiring high-quality pulse to ensure measurement accuracy. Whereas, EIS analyze resistance on the basis of impedance spectrum. It is highly precise, but only suitable in laboratory due to the necessity for special equipment.

Given the weakness of current-pulse technique and EIS, Kalman filter-based parameter estimation methods have aroused abundant research attention recently. Those approaches attain optimal state estimation from measured parameters including voltage, current, and temperature. Plett et al. [12–14] firstly estimate battery parameter using Extended Kalman filter and acquire accurate estimation results. Tian et al. [15] estimate battery SOC and capacity through UKF. Than Lim et al. [16] estimate electric vehicles battery parameters by Fading Kalman filter. In those Kalman filter methods, the system state equation has three types of lithium-ion battery model in general, i.e. electrochemical model, mathematical model, and electrical model [17]. Mathematical model has fastest operation, and yet lower accuracy and applicability. Electrical model is much simpler compared with electrochemical model. It can be applied into comprehensive system-level dynamic models and track how battery responds to transient loads with high accuracy. Unfortunately, this model requires the correlation between OCV and SOC which is hard to obtain in practice. To address this problem, Wei et al. [18] use a function to describe OCV in capacity estimation, yet it may not be suitable for aging battery. To suit for aging battery, Lavigne et al. [19] propose an OCV curve adjustment algorithm with aging, but this method is difficult to apply in on-orbit satellite because it needs at least two OCV measurements in normal operation or in specific operation (for instance, charge phase).

Electrochemical model has no need for OCV-SOC curve, and encompasses transport phenomena and electrochemical kinetics. This model is very accurate due to the development of electrochemical theory, whereas it needs sophisticated battery parameters for estimation. Accordingly, to avoid that constant OCV-SOC curve is employed to estimate battery parameters under different SOHs, a resistance estimation method using simplified electrochemical model is proposed herein. Through this model, resistance as health index is estimated accurately during battery aging process.

## 2 Relationships Between Resistance and Capacity

Establishing relationships between SOH and internal resistance lays the foundation for estimating SOH by internal resistance. The primary ageing mechanisms of battery lies on the loss of active lithium [20]. Lithium is primarily consumed with the growth of solid electrolyte interphase (SEI) which consequently increases resistance [21]. The SEI layer is assumed to be homogeneous, and the ionic conductivity  $\kappa_{SEI}$  is constant. Thus, the resistance at the SEI film can be noticed as [22]:

$$R_{SEI} = \frac{\delta_{film}}{\kappa_{SEI}} \quad (1)$$

Where  $\delta_{SEI}$  is the thickness of SEI film and can be calculated through equation below:

$$\frac{d\delta_{film}}{dt} = -\frac{i_s}{2F} \frac{M_{SEI}}{\rho_{SEI}} \quad (2)$$

Where  $F$  is Faraday's constant,  $M_{SEI}$  is molecular weight of SEI, while  $\rho_{SEI}$  represents for SEI density, and  $i_s$  is the side-reaction current density referred to as interfacial surface area of anode. The time integral of  $i_s$  is the mount of loss of active lithium  $q_{loss}$ . Then the  $R_{SEI}$  can be noted that:

$$R_{SEI} = \int_0^t \delta_{film}/\kappa_{SEI} dt = R_0 - K_1 q_{loss} \quad (3)$$

Then  $K_1 = M_{SEI}/2F\rho_{SEI}\kappa_{SEI}$

Following Daigle's model [23], the capacity of battery decreases linearly with the  $q_{loss}$ .

$$Q_t = Q_0 - K_2 q_{loss} \quad (4)$$

Where,  $Q_t$  is capacity in current time,  $Q_0$  is initial capacity,  $K_2$  is the coefficient.

This relationship is also verified by simulating the degradation of battery performance. The simulation is implemented in Comsol Multiphysics 5.2a and the results are presented in Fig. 1:

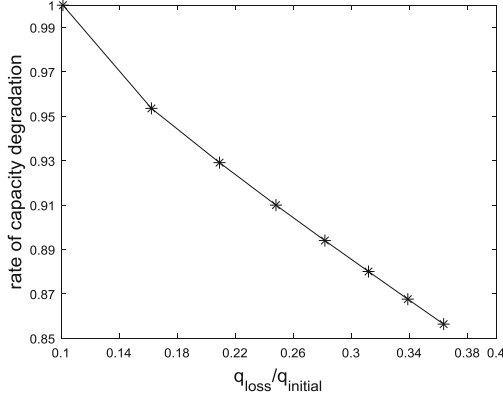


**Fig. 1.** Correlation of capacity and  $q_{loss}/q_{initial}$

Accordingly, the relationship between resistance  $R$  and capacity loss  $Q_{loss}$  can be expressed as:

$$Q_{loss} = \alpha R - \beta \quad (5)$$

Where  $\alpha$ ,  $\beta$  denoted as the coefficient.

The traditional battery SOH is defined by battery capacity [10]

$$SOH = \frac{Q_t - Q_{end}}{Q_0 - Q_{end}} \quad (6)$$

Taking Eqs. (5) to (6)

$$SOH = \frac{R_{end} - R_t}{R_{end} - R_0} \quad (7)$$

Where  $R_t$  is current resistance,  $R_0$  is resistance at start of the lifetime and  $R_{end}$  is resistance at end of the lifetime.

### 3 Resistance Estimate Method

#### 3.1 Li-Ion Battery Discharge Model

Pseudo-two-dimensional (P2D) model, a frequently employed electrochemical model, describes the internal behavior of lithium-ion following concentrated solution theory. The sandwich structure of lithium-ion encompasses positive and negative porous

electrodes, a separator and a current collector [24]. Then, lithium ions (Li+) can diffuse between positive and negative electrodes, and intercalate and deintercalate from active materials in different electrodes during charge or discharge processes. Under P2D model, battery model originates from a simplified set of electrochemical equations about charge flow and voltage drops at the cathode, anode, and separator layers of a Li-ion battery. This model is elucidated by Daigle [23] and summarized by Bole [25]. Herein, Daigle’s model is adopted and modified to estimate the state of age-dependent resistance according to current-voltage dynamics of batteries in operation.

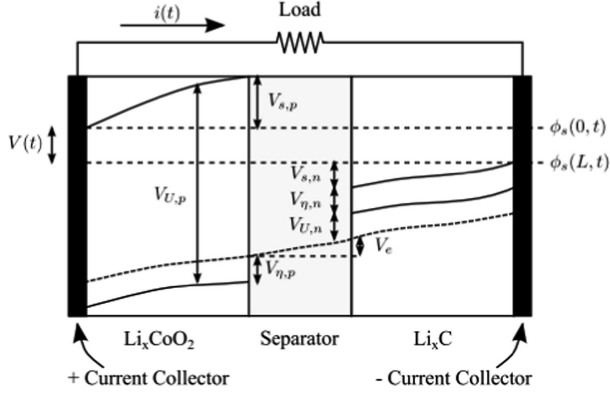


**Fig. 2.** Battery voltage [23]

As shown in Fig. 2, pressure drop  $V(t)$  of overall battery voltage is potential difference between positive current collector  $\phi_s(0,t)$  and negative current collector  $\phi_s(L,t)$  minus pressure drop caused by internal resistance at the current collectors, which is not diagramed.  $V(t)$  is superposed by voltage drops though further analysis and research about all parts of the battery. The equilibrium potential is  $V_{U,p}$  at the positive current collector (subscript  $p$ ). This voltage is then reduced by the solid-phase ohmic overpotential  $V_{s,p}$  and the surface overpotential  $V_{\eta,p}$ . The electrolyte ohmic resistance then causes another drop  $V_e$ . There are additionally voltage drops caused separately by surface overpotential  $V_{\eta,n}$  and solid-phase ohmic overpotential  $V_{s,n}$  at the negative electrode (subscript  $n$ ). Eventually, the voltage drops again, which is attributed to the equilibrium potential  $V_{U,n}$  at the negative current collector. The resistance at current collector also causes voltage drop  $V_{cc,p}$  and  $V_{cc,n}$ . All the voltage drops derived from resistance ( $V_{cc,p}$ ,  $V_{s,p}$ ,  $V_e$ ,  $V_{s,n}$ ,  $V_{cc,n}$ ) can be lumped together:

$$\begin{aligned}
 V_0 &= V_{cc,p} + V_{s,p} + V_e + V_{s,n} + V_{cc,n} \\
 &= i_{app}(R_{cc,p} + R_{s,p} + R_e + R_{s,n} + R_{cc,n}) \\
 &= i_{app}R_0
 \end{aligned} \tag{8}$$

Each electrode, either positive or negative, is split into two volumes, i.e. a surface layer (subscript  $s$ ) and a bulk layer (subscript  $b$ ), respectively. These voltage terms of

battery are expressed as functions of the amount of charge in the electrodes and the equations are described by the set of equations below:

$$V = V_{U,p} - V_{U,n} - V_0 - V'_{\eta,p} - V'_{\eta,n} \quad (9)$$

$$V_{U,i} = U_0 + \frac{RT}{nF} \ln \left( \frac{1 - x_{s,i}}{x_{s,i}} \right) + V_{INT,i} \quad (10)$$

$$V_{INT,i} = \frac{1}{nF} \left( \sum_{k=0}^{N_i} A_{i,k} \left( (2x_i - 1)^{k+1} - \frac{2x_i k (1 - x_i)}{(2x_i - 1)^{1-k}} \right) \right) \quad (11)$$

$$V_{\eta,i} = \frac{RT}{F\alpha} \operatorname{arcsinh} \left( \frac{J_i}{2J_{i0}} \right) \quad (12)$$

$$J_i = i_{app} / S_i \quad (13)$$

$$J_{i0} = k_i (1 - x_{s,i})^a (x_{s,i})^{1-a} \quad (14)$$

$$V'_0 = i_{app} R_0 \quad (15)$$

$V'_{\eta,p}, V'_{\eta,n}$  is observed value, and  $V_{\eta,p}, V_{\eta,n}$  is actual value which change instantaneously. Their relationship can be expressed by parameter of empirical time constants  $\tau_{\eta,i}$ .

$$\dot{V}'_{\eta,p} = \left( V_{\eta,p} - V'_{\eta,p} \right) / \tau_{\eta,p} \quad (16)$$

$$\dot{V}'_{\eta,n} = \left( V_{\eta,n} - V'_{\eta,n} \right) / \tau_{\eta,n} \quad (17)$$

Where the subscript  $i$  is electrode, where  $i = n$  or  $i = p$ .  $U_0$  is a reference potential,  $R$  is the universal gas constant, while  $T$  is the electrode temperature (in K), and  $n$  is the number of electrons transferred in the reaction ( $n = 1$  for Li-ion),  $F$  is Faraday's constant, and  $V_{INT,i}$  is denoted as the activity correction term (0 in the ideal condition). The Redlich-Kister expansion is employed with  $N_p=12$  and  $N_n=0$  [23].  $i_{app}$  is the applied electric current.  $J_i$  represents for the current density, and  $J_{i0}$  is the exchange current density,  $k_i$  is a lumped parameter of several constants, including rate coefficient, electrolyte concentration, and maximum ion concentration.

Each electrode, either positive or negative, is split into two individual control volumes (CVs), i.e. a surface layer (subscript s) and a bulk layer (subscript b), respectively. The mole fractions ( $x_i, x_{s,i}, x_{b,i}$ ) can be expressed by equations below:

$$x_i = q_i / q^{\max}; \quad x_{s,i} = q_{s,i} / q_{s,i}^{\max}; \quad x_{b,i} = q_{b,i} / q_{b,i}^{\max} \quad (18)$$

Where  $q_i$  is the amount of charge in electrode  $i$ ,  $q_{s,i}$  is the amount of charge in surface of electrode  $i$ ,  $q_{b,i}$  is the amount of charge in bulk of electrode  $i$ . Abiding by the principle of charge move in these volumes, the charge ( $q$ ) variables are expressed as following differential equations:

$$\dot{q}_{s,p} = i_{app} + \dot{q}_{bs,p} \quad (19)$$

$$\dot{q}_{b,p} = -\dot{q}_{bs,p} + i_{app} - i_{app} \quad (20)$$

$$\dot{q}_{s,n} = -i_{app} + \dot{q}_{bs,n} \quad (21)$$

$$\dot{q}_{b,n} = -\dot{q}_{bs,n} + i_{app} - i_{app} \quad (22)$$

The term  $\dot{q}_{bs,i}$  expresses diffusion from the bulk to surface layer for electrode  $i$  and the express as follows:

$$\dot{q}_{bs,i} = (c_{b,i} - c_{s,i})/D \quad (23)$$

Where  $D$  is the diffusion constant. The  $c$  terms are lithium ion concentrations:

$$c_{b,i} = q_{b,i}/v_{b,i}; \quad c_{s,i} = q_{s,i}/v_{s,i} \quad (24)$$

Where, for CV  $v$  in electrode  $i$ ,  $c_{v,i}$  is the concentration of charge in electrode  $i$ , and  $v_{v,i}$  is the volume of CV. Note  $v_i = v_{b,i} + v_{s,i}$  and the following relations:

$$q_p = q_{s,p} + q_{b,p} \quad (25)$$

$$q_n = q_{s,n} + q_{b,n} \quad (26)$$

$$q^{\max} = q_{s,p} + q_{b,p} + q_{s,n} + q_{b,n} \quad (27)$$

$$q_{s,i}^{\max} = q^{\max} \frac{v_{s,i}}{v_i} \quad (28)$$

Considering that this model is used to estimate resistance with aging, the variation of parameter with aging cannot be neglected. At present, there are three commonly reported degradation modes [26]: (1) loss of lithium inventory, (2) loss of active material in positive electrode, (3) loss of active material in negative electrode. Those degradation modes in this work appear as the decrease of maximum charge amount. The decay trajectory of the maximum amount of charge can be estimated by a linear model [27]:

$$q^{\max} = q_0^{\max} - a \cdot N_{cyc} \quad (29)$$

Where  $a$  is lithium ions loss coefficient,  $N_{cyc}$  is number of cycle.

In summary, this model involves as states  $q_{s,p}, q_{b,p}, q_{b,n}, q_{s,n}, R_0, V'_{\eta,p}, V'_{\eta,n}$ . The model output is denoted by  $V$ . Parameter values for a typical 18650 Li-ion cells are given in Daigle's literature [23]. In this model, the  $R_0$  is variable to be estimated, differing from Bole's literature [25].

### 3.2 UKF Framework

Kalman filter is mathematical technique which offers an efficient recursive means to estimate the states of a process and ultimately minimize the mean of the squared error [28]. For the highly nonlinear electrochemical battery model, UKF is more accurate than KF or EKF [29, 30]. This chapter summarize the filter basics to be mentioned, and more details may be found in Haykin's book [31].

The battery model is sophisticated and on-board measurement may not be very accurate. Therefore, noise items should be involved for both the process model and measurement model. The covariance of the process noise is assumed as  $R_p$ , associated with the system noise and current measurement error, while the covariance of the measurement noise is  $R_m$ , associated with the terminal voltage measurement error. The steps of applying the UKF to estimate resistance are summarized as follows.

Step1. Initialize the state and covariance for every discharge test date.

Step2. Calculate the weighted sigma points:

$$S = \{w_i, X_i; i = 0, 1, \dots, 2L\} \quad (30)$$

where the sigma points are:

$$X_0 = \hat{x}_{k-1} \quad (31)$$

$$X_i = x + \left( \sqrt{(L + \lambda) P_{k-1}^x} \right)_i, i = 1, 2, \dots, L \quad (32)$$

$$X_i = x - \left( \sqrt{(L + \lambda) P_{k-1}^x} \right)_i, i = L + 1, L + 2, \dots, 2L \quad (33)$$

where the parameter  $\lambda = \alpha^2(L + \kappa) - L$  and the weights  $w_i$  can be calculated by the equations below:

$$w_0^m = \lambda / (L + \lambda) \quad (34)$$

$$w_0^c = \lambda / (L + \lambda) + (1 - \alpha^2 + \beta) \quad (35)$$

$$w_i^m = w_i^c = 1 / (2(L + \lambda)), i = 1, \dots, 2L \quad (36)$$

where the  $\alpha, \beta$  is parameter for unscented transform. In this paper, the common parameters  $\alpha = 1, \beta = 0, \kappa = 0$  are adopted.



Step3. Update each sigma point via the time-update equation to predict the system state and calculate the covariance of the estimated state

$$X_{k|k-1} = h(X_{k-1}, u_k) + R_p \quad (37)$$

$$x_k^- = \sum_{i=0}^{2L} w_i^m X_{i,k|k-1} \quad (38)$$

$$P_k^{x-} = \sum_{i=0}^{2L} w_i^c (X_{i,k|k-1} - x_k^-) (X_{i,k|k-1} - x_k^-)^T \quad (39)$$

Step4. Update the measurement as followed:

$$Y_{k|k-1} = g(X_{k|k-1}, u_k) + R_m \quad (40)$$

$$y_k^- = \sum_{i=0}^{2L} w_i^m Y_{i,k|k-1} \quad (41)$$

$$P_k^{y-} = \sum_{i=0}^{2L} w_i^c (Y_{i,k|k-1} - y_k^-) (Y_{i,k|k-1} - y_k^-) \quad (42)$$

$$P_k^{xy-} = \sum_{i=0}^{2L} w_i^c (X_{i,k|k-1} - x_k^-) (Y_{i,k|k-1} - y_k^-) \quad (43)$$

$$K_k = P_k^{xy-} (P_k^{yy-})^{-1} \quad (44)$$

Step5. Update the state and covariance as followed:

$$\hat{x}_k = x_k^- + K_k (y_k - y_k^-) \quad (45)$$

$$P_k^x = P_k^{x-} - K_k P_k^{y-} K_k^T \quad (46)$$

For the resistance estimation in this paper, observe various is  $V$  and state variable of UKF include  $V_0, V'_{\eta,p}, V'_{\eta,n}, q_{b,n}, q_{s,n}, q_{b,p}, q_{s,p}$ . The state equation consists of Eqs. (6) and (10–26) and observe equation consist of Eqs. (7–9). The parameters of battery vary slightly in one discharge cycle, inclusive of  $q^{\max}, D$  [32]. Accordingly, the parameters are assumed being constant for each discharge cycle except for resistance in single discharge. Besides,  $q^{\max}$  change with cycle and the value can be obtain from Eq. (27).

## 4 Resistance Estimation Algorithm Verification

### 4.1 Experimental Data Source

This work employs public battery life test data originating from Prognostics CoE at the U.S. National Aeronautics and Space Administration (NASA) Ames to verify the resistance estimation algorithm for different SOHs. As Fig. 3 shows, experimental setup primarily consists of a set of Li-ion cells which may reside either inside or outside

an environmental chamber, chargers, loads, EIS equipment for battery health monitoring (BHM), a suite of sensors (i.e. voltage, current and temperature), some custom switching circuitry, data acquisition system and a computer for control and analysis. The experiments are operated through 3 different operational profiles (i.e. charge, discharge and EIS) at ambient temperature, 23 °C. Charging is performed in CC-CV mode at 1.5 A. Discharging is performed at a constant current level of 2 A until cut-off voltage. The charge and discharge continue to loop until the capacity degraded to 30% of rated capacity. Data set B0006 is adopted here.

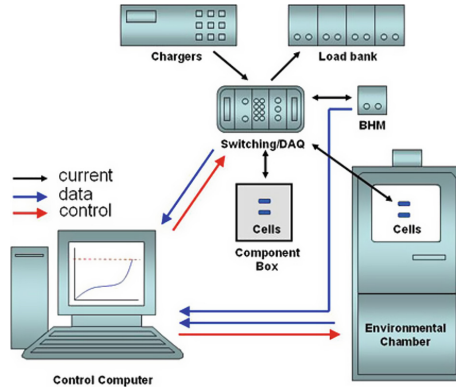


Fig. 3. The experimental setup schematic diagram.

## 4.2 Verification Through Battery Degradation Data

Without loss of generality, complete life test data of B0006 battery is employed. B0006 data set involves 616 operational profiles (168 discharge profiles and 141 EIS after charging completes). Measurement encompasses battery current, terminal voltage, surface temperature and stationary resistance. For each discharge profile, current and temperature serve as controlled quantity, and terminal voltage serves as observed quantity for UKF algorithm. Battery parameters are critical for resistance estimation. In this paper, lithium ions loss coefficient  $a$  is 30, and other battery parameters are given by Daigle [23], as summarized in Tables 1 and 2.

Internal resistance varies with SOC [33, 34], and the correlation between ohmic internal resistance and SOC is presented in Fig. 4, originating from battery test data of UR 18650ZY. As suggested in the test data, the resistance decreased at initial discharge and rose rapidly at the end of discharge. For each discharge profile, this law is consistent with estimated results of the resistance, and one estimated result is illustrated in Fig. 5. To compare with the internal resistance from EIS, the mean of estimated values from UKF during overall process of single charge is denoted as the estimated value of battery resistance. Then, the mean of EIS measurements at full charge discharge states is employed as the actual value of battery resistance.

**Table 1.** Battery parameters

Parameter	Value
$q_0^{max}$	$1.32 \times 10^4$ C
$R$	8.314 J/mol/K
$T$	292 K
$F$	96487 C/mol
$n$	1
$D$	$7 \times 10^6$ mol s/C/m <sup>3</sup>
$\tau_0$	10 s
$\alpha$	0.5
$R_0$	0.085 $\Omega$
$S_p$	$2 \times 10^{-4}$ m <sup>4</sup>
$k_p$	$2 \times 10^4$ A/m <sup>3</sup>
$v_{s,p}$	$2 \times 10^{-6}$ m <sup>3</sup>
$v_{b,p}$	$2 \times 10^{-5}$ m <sup>3</sup>
$\tau_{\eta,p}$	90 s
$S_n$	$2 \times 10^{-4}$ m <sup>4</sup>
$k_n$	$2 \times 10^4$ A/m <sup>3</sup>
$v_{s,n}$	$2 \times 10^{-6}$ m <sup>3</sup>
$v_{b,n}$	$2 \times 10^{-5}$ m <sup>3</sup>
$\tau_{\eta,n}$	90 s

**Table 2.** Battery activity correction term coefficient

Parameter	Value
$U_{0,p}$	4.03 V
$A_{p,0}$	-33642.23 J/mol
$A_{p,1}$	0.11 J/mol
$A_{p,2}$	23506.89 J/mol
$A_{p,3}$	-75679.26 J/mol
$A_{p,4}$	14359.34 J/mol
$A_{p,5}$	307849.79 J/mol
$A_{p,6}$	85053.13 J/mol
$A_{p,7}$	-1075148.06 J/mol
$A_{p,8}$	2173.62 J/mol
$A_{p,9}$	991586.68 J/mol
$A_{p,10}$	283423.47 J/mol
$A_{p,11}$	-163020.34 J/mol
$A_{p,12}$	-470297.35 J/mol
$U_{0,n}$	0.01 V
$A_{n,0}$	-86.19 J/mol

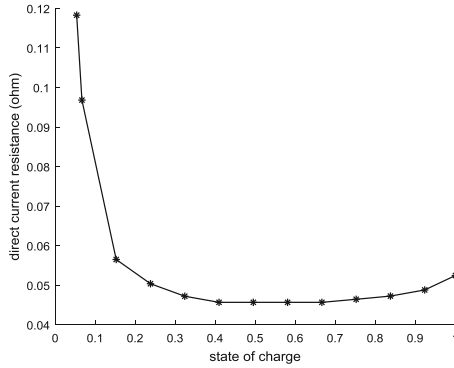


Fig. 4. The correlation of ohmic internal resistance and SOC at 1C

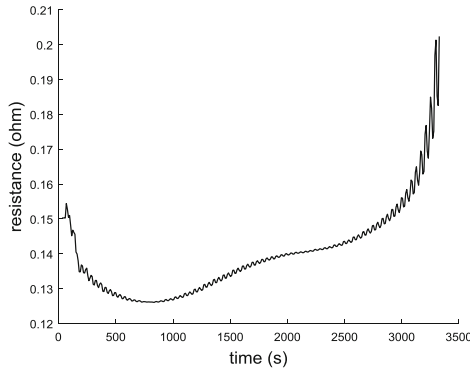
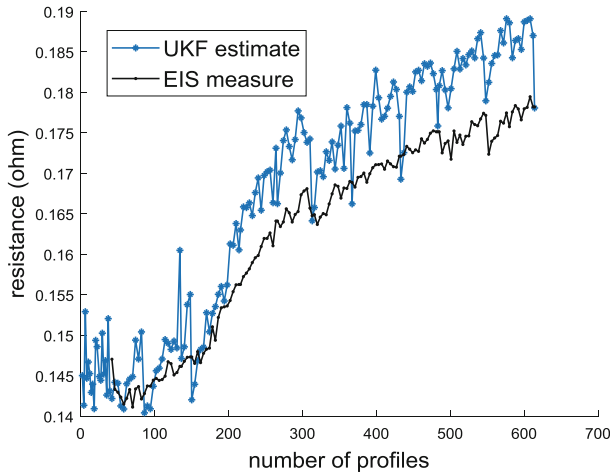
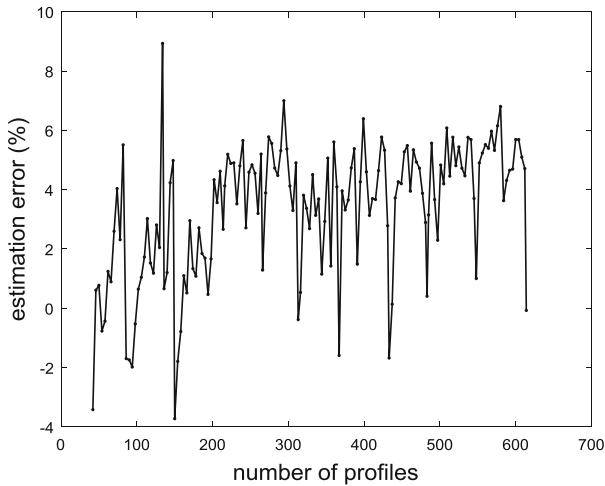


Fig. 5. Resistance estimate result for one of discharge profiles.

The ohmic internal resistance is estimated, and the actual ohmic internal resistance is equal to the sum of  $R_{ct}$  and  $R_e$  according to the battery model in Sect. 3.1 [7]. Comparison results of actual and estimated resistance in all degradation processes are plotted in Fig. 6, and the estimation errors are plotted in Fig. 7 to verify the estimated results. The estimated results are found very close to actual resistance, and maximum estimate error is under 10%. In first 80 discharges, the estimated resistance estimation does not vary apparently as new lithium battery needs some charge-discharge cycles to complete activation. Then, the resistance increases progressively with the degeneration of battery. By analyzing overall degradation process, estimated internal resistance is approximate 5% greater than measured value from EIS. This phenomenon is associated with the simplification of the models. For instance, a constant is adopted to replace  $D$ . In normal conditions,  $D$  changes with SOC and SOH. And the actual  $D$  change rule and the impact on estimation result is to be majorly studied in the future.



**Fig. 6.** Resistance estimation results at different degradation



**Fig. 7.** Resistance estimation error at different degradation

The linear relationship between resistance and capacity is proved by these estimation results as well. As Fig. 8 presents, the relationship between resistance estimation results and capacity loss satisfies the linear rule well except in first 80 discharges. Data of Fig. 8 are fitted through Eq. 44. Thus, the battery state of health can be expressed by resistance very well R-square: 0.9992.

$$Q_{loss} = 15.151 * R - 2.0347 \quad (47)$$

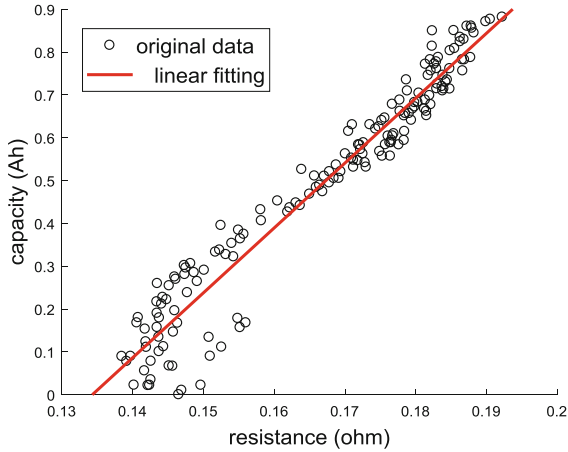


**Fig. 8.** Capacity loss of B0006 battery with different resistance

## 5 Conclusion

In this paper, UKF-based battery resistance estimation technique is developed and validated experimentally using B0006 battery from NASA. Then, the linear relationship between resistance and capacity loss is deduced and validated. Accordingly, this technique can be applied to estimate SOH. To estimate the resistance, a simplified electrochemical model is adopted to express the changes of battery voltage. This model could express the battery dynamics approximately, and OCV-SOC curve varied with battery degeneration is not required. Besides, the impact of temperature and parameter changes with aging has also been considered in this model. Thus, this algorithm can estimate battery resistance under different SOH and different conditions more accurately. Moreover, this technique does not require full discharge data. Hence, the proposed method is appropriate for satellite battery health monitoring with unfixed operating current and depth of discharge. For further work, the change of charge amount and diffusion coefficient with battery degeneration will be considered for more accurate estimation.

## References

1. Wang, D., Li, G.X., Pan, Y.L.: The technology of lithium ion batteries for spacecraft application. *Aerosp. Shanghai* **17**, 54–59 (2000)
2. Ping, L., Ling-Sheng, T., Jie, W., Ya-Lin, L., Zhen-Hai, C.: Application of li-ion battery in GEO satellite. *Chin. J. Power Sources* 1–2 (2018)
3. Bercibar, M., et al.: Online state of health estimation on NMC cells based on predictive analytics. *J. Power Sources* **320**, 239–250 (2016)
4. Yang, J., Xia, B., Huang, W., Fu, Y., Mi, C.: Online state-of-health estimation for lithium-ion batteries using constant-voltage charging current analysis. *Appl. Energ* **212**, 1589–1600 (2018)

5. Yang, Q., Xu, J., Cao, B., Xu, D., Li, X., Wang, B.: State-of-health estimation of lithium-ion battery based on interval capacity. *Energy Procedia* **105**, 2342–2347 (2017)
6. Zheng, L., Zhu, J., Lu, D.D., Wang, G., He, T.: Incremental capacity analysis and differential voltage analysis based state of charge and capacity estimation for lithium-ion batteries. *Energy* **150**, 759–769 (2018)
7. Li, Y., et al.: A quick on-line state of health estimation method for Li-ion battery with incremental capacity curves processed by Gaussian filter. *J. Power Sources* **373**, 40–53 (2018)
8. Wang, L., Pan, C., Liu, L., Cheng, Y., Zhao, X.: On-board state of health estimation of LiFePO<sub>4</sub> battery pack through differential voltage analysis. *Appl. Energ.* **168**, 465–472 (2016)
9. Maheshwari, A., Heck, M., Santarelli, M.: Cycle aging studies of lithium nickel manganese cobalt oxide-based batteries using electrochemical impedance spectroscopy. *Electrochim. Acta* **273**, 335–348 (2018)
10. Chen, L., Lü, Z., Lin, W., Li, J., Pan, H.: A new state-of-health estimation method for lithium-ion batteries through the intrinsic relationship between ohmic internal resistance and capacity. *Measurement* **116**, 586–595 (2018)
11. Cui, Y., et al.: State of health diagnosis model for lithium ion batteries based on real-time impedance and open circuit voltage parameters identification method. *Energy* **144**, 647–656 (2018)
12. Plett, G.L.: Extended Kalman filtering for battery management systems of LiPB-based HEV battery packs - Part 1. Background. *J. Power Sources* **134**, 252–261 (2004)
13. Plett, G.L.: Extended Kalman filtering for battery management systems of LiPB-based HEV battery packs - Part 2. Modeling and identification. *J. Power Sources* **134**, 262–276 (2004)
14. Plett, G.L.: Extended Kalman filtering for battery management systems of LiPB-based HEV battery packs - Part 3. State and parameter estimation. *J. Power Sources* **134**, 277–292 (2004)
15. Tian, Y., Xia, B., Sun, W., Xu, Z., Zheng, W.: A modified model based state of charge estimation of power lithium-ion batteries using unscented Kalman filter. *J. Power Sources* **270**, 619–626 (2014)
16. Lim, K., Bastawrous, H.A., Duong, V., See, K.W., Zhang, P., Dou, S.X.: Fading Kalman filter-based real-time state of charge estimation in LiFePO<sub>4</sub> battery-powered electric vehicles. *Appl. Energ.* **169**, 40–48 (2016)
17. Cao, Y., Kroeze, R.C., Krein, P.T.: Multi-timescale parametric electrical battery model for use in dynamic electric vehicle simulations. *IEEE Trans. Transp. Electrification* **2**, 432–442 (2016)
18. Wei, Z., Zhao, J., Ji, D., Tseng, K.J.: A multi-timescale estimator for battery state of charge and capacity dual estimation based on an online identified model. *Appl. Energ.* **204**, 1264–1274 (2017)
19. Lavigne, L., Sabatier, J., Francisco, J.M., Guillemard, F., Noury, A.: Lithium-ion Open Circuit Voltage (OCV) curve modelling and its ageing adjustment. *J. Power Sources* **324**, 694–703 (2016)
20. Cao, W., Li, J., Wu, Z.: Cycle-life and degradation mechanism of LiFePO<sub>4</sub>-based lithium-ion batteries at room and elevated temperatures. *Ionics* **22**, 1791–1799 (2016)
21. Spotnitz, R.: Simulation of capacity fade in lithium-ion batteries. *J. Power Sources* **113**, 72–80 (2003)
22. Safari, M., Morcrette, M., Teyssot, A., Delacourt, C.: Multimodal physics-based aging model for life prediction of li-ion batteries. *J. Electrochem. Soc.* **156**(3), A145–A153 (2009)
23. Daigle, M., Kulkarni, C.S.: Electrochemistry-based battery modeling for prognostics. In: Conference of the Prognostics and Health Management Society (2013)

24. Ramadesigan, V., Northrop, P.W.C., De, S., Santhanagopalan, S., Braatz, R.D., Subramanian, V.R.: Modeling and simulation of lithium-ion batteries from a systems engineering perspective. *J. Electrochem. Soc.* **159**, R31–R45 (2012)
25. Bole, B., Kulkarni, C.S., Daigle, M., Kulkarni, C.S.: Adaptation of an electrochemistry-based li-ion battery model to account for deterioration observed under randomized use. In: Conference of the Prognostics and Health Management Society (2014)
26. Birkl, C.R., Roberts, M.R., McTurk, E., Bruce, P.G., Howey, D.A.: Degradation diagnostics for lithium ion cells. *J. Power Sources* **341**, 373–386 (2017)
27. Xiong, R., Li, L., Li, Z., Yu, Q., Mu, H.: An electrochemical model based degradation state identification method of Lithium-ion battery for all-climate electric vehicles application. *Appl. Energ* **219**, 264–275 (2018)
28. He, H., Xiong, R., Guo, H.: Online estimation of model parameters and state-of-charge of LiFePO<sub>4</sub> batteries in electric vehicles. *Appl. Energ* **89**, 413–420 (2012)
29. Li, J., Klee Barillas, J., Guenther, C., Danzer, M.A.A.: A comparative study of state of charge estimation algorithms for LiFePO<sub>4</sub> batteries used in electric vehicles. *J. Power Sources* **230**, 244–250 (2013)
30. He, Y., Liu, X., Zhang, C., Chen, Z.: A new model for State-of-Charge (SOC) estimation for high-power Li-ion batteries. *Appl. Energ* **101**, 808–814 (2013)
31. Haykin, S.: Kalman Filtering and Neural Networks. Adaptive & Learning Systems for Signal Processing Communications & Control, pp. 170–174 (2001)
32. Daigle, M., Kulkarni, C.S.: End-of-discharge and end-of-life prediction in lithium-ion batteries with electrochemistry-based aging models. In: AIAA Infotech@Aerospace Conference (2015)
33. Chen, M., Rincon-Mora, G.A.: Accurate electrical battery model capable of predicting, runtime and I-V performance. *IEEE Trans. Energy Convers.* **21**, 504–511 (2006)
34. Ning, G., Haran, B., Popov, B.N.: Capacity fade study of lithium-ion batteries cycled at high discharge rates. *J. Power Sources* **117**, 160–169 (2003)